ISSN 1070-3284, Russian Journal of Coordination Chemistry, 2020, Vol. 46, No. 8, pp. 584–591. © Pleiades Publishing, Ltd., 2020.

5-Fluorouracil Trapping in a Porous Ba(II)-Organic Framework: Drug Delivery and Anti-Thyroid Cancer Activity Evaluation

Q. J. Zhang[a], J. K. Zhao[a], Y. Li[a], X. Y. Wu[a], L. L. Ma[a], and Z. M. Ding[a, *]

[a] *Department of General Surgery, Xuzhou Central Hospital, Xuzhou, Jiangsu, China*

**e-mail: ziming_ding666@126.com*

Received May 27, 2019; revised June 28, 2019; accepted September 12, 2019

Abstract—Solvothermal treatment of $Ba(NO_3)_2$ with the rigid tricarboxylic acid linker 4,4',4"-s-triazine-2,4,6-triyltribenzoic acid (H_3TATB) in a mixture of H_2O and *N*,*N*-dimethylformamide (DMF) produces a new three-dimensional porous metal-organic framework having the chemical formula of $[Ba(HTATB)(H_2O)_2](DMF)_4$ (**I**). The complex **I** has been characterized by powder X-ray diffraction, elemental analysis and single crystal X-ray diffraction (CIF file CCDC no. 1898532). In light of its large inner spaces as well as widely distributed open metal sites, the guest-free **I** (**Ia**) has been used as a crystalline vessel for trapping the anticancer drug 5-fluorouracil (5-FU), which has been investigated both experimentally and computationally. Furthermore, MTT assay was employed to evaluate the in vitro cytotoxicity of the carrier 5-FU loaded **Ia** against the human thyroid cancer cell lines.

Keywords: Ba(II)-organic framework, crystal structure, 5-FU encapsulation, anticancer activity

DOI: 10.1134/S1070328420080072

INTRODUCTION

Although great achievements have been realized in the feild of biological medicine, cancer is still the leading killer which results in millions of people death every, especially in the developing and the undeveloped countries [1]. To data, chemotherapy is still one of the most effective and widely used treatment method for cancer [2]. However, the intrinsic shortcomings of the traditional anticancer drugs such as poor pharmacokinetics, undesirable side effects and non-specificity make these anticancer drugs poor efficiency when they are used for treating the targeted cancer cells, which also limit their large does of direct administration to patients [3]. To address the arisen clinical shortcomings of the traditional chemotherapeutic drugs, the scientists in the feilds of chemistry and biology have tried their best to develop new treatment method for cancer with enhanced therapeutic efficacy and reduced side effects. In this case, the drug delivery systems (DDSs) using the nano porous carriers for encapsulation of anticancer agents have received considerable attention because they could release anticancer drugs without "burst effect" and keep the drug concentration stably in the targeted issues [4].

As a class of widely explored crystal materials with nanoporous spaces constructed from metal ions/clusters and organic ligands, metal-organic frameworks (MOFs) have gained substantial research efforts during last two decades [5]. The nanoporous spaces of MOFs could be finely modulated via selection of suitable organic ligands and metal ions for the targeted applications, and various functional sites could be also be embedded in these nanoporous spaces via the post-modification [6]. The high pore volume and tunable pore size/surroundings endow MOFs with great advantages which could be applied in the field of gas separating, catalyzing, sensing and anticancer drug delivery [7–11]. The above-mentioned advantages of MOFs also catch the attention of scientists in the field of biomedicine, which is evidenced by the large amount of porous MOFs developed as crystalline flask to achieve advanced drug delivery systems [12]. The first MOF-based drug delivery system has been achieved by Férey and co-workers, who have showed that the MIL-53 with Fe^{3+} and Cr^{3+} metal centers could be used as crystalline flask for trapping and releasing of Ibuprofen [13]. To realize different biological applications such as biomedicine, imaging and biosensing, the corresponding biocompatibility should be considered. Although some coordination polymers could house a large capacity of drug molecules, their metal centers such as Cr^{3+}, Cd^{2+} and Ni^{2+} are highly toxic to the human beings [14]. In this work, concerning cytotoxicity of the drug carrier, we adopt the metal cation Ba^{2+} (the barium compounds are usually nontoxic when are insoluble) and an organic carboxylic ligand 4,4',4"-s-triazine-2,4,6-triyltribenzoic acid (H_3TATB) to construct a new three-dimensional Ba(II)-based coordination polymer, namely

$[Ba(HTATB)(H_2O)_2](DMF)_4$ (**I**) by reaction of $Ba(NO_3)_2$ and H_3TATB in the mixture of H_2O and *N*,*N*-dimethylformamide (DMF) at 120°C. Complex **I** has been characterized by powder X-ray diffraction (PXRD), elemental analysis (EA) and single crystal X-ray diffraction (SCXRD). Furthermore, we use the GCMC simulation to probe the sorption performance of the solvent-free **I** toward the anticancer drug 5-fluorouracil (5-FU), which shows that this coordination polymer could take up considerable amount of 5-FU with a moderate strong framework-guest interaction. Finally, MTT assay was used to access the in vitro cytotoxicity of the carrier **I** and 5-FU loaded **Ia** against three human thyroid cancer cells (FTC-133, BC-PAP and SW579).

EXPERIMENTAL

Apparatus and materials. Unless otherwise mentioned, all the chemicals and solvents used in this study were brought from the Beijing Beijing Ouhe Chemical Reagent company and used without further manipulation. The Elementary Vario EL III instrument (made in German) was used to acquire the H, C and N content in the as-prepared complex **I**. A Rigaku Mini Flex-II X-ray (Japan) equipped with CuK_α radiation was used to measure the PXRD profiles. Thermogravimetric (TGA) curve of complex **I** was collected on a Netzsch Model STA 449C thermal analyzer with a heating rate of 10°C/min under N_2 atmosphere. The UV-Vis spectra for the 5-FU solution were determined using a JASCO V-530 spectrometer. Gas adsorption of CO_2 was measured on an ASAP 2020 gas adsorption analyzer (Micromeritics). Before adsorption, all samples (~50 mg) were activated in fresh acetone and then degassed at 413 K for 10 h. Helium gas was used for estimation of the dead volume. The dry ice was used to control the temperature in the CO_2 sorption process.

Synthesis complex I. A mixture H_3TATB (0.2 mmol, 87 mg), $Ba(NO_3)_2$ (0.2 mmol, 52 mg), DMF (6 mL), and water (4 mL) was added into a clean glass vial. The solution was dealt with ultrasonic treatment and then kept at 373 K in an oven for 3 days. Colorless crystalline products of were produced, cleaned by EtOH and left in the air to make them dried. The yield of **I** was 76% on the basis of the H_3TATB ligand used.

For $C_{36}H_{44}N_7O_{12}Ba$ (**I**)

Anal. calcd., %	C, 47.83	H, 4.91	N, 10.84
Found, %	C, 47.51	H, 4.69	N, 10.26

X-ray crystal structure determination. The intensity data for the complex **I** were collected using the graphite monochromatic CuK_α (λ = 1.54184 Å) of the Nonius/Kappa CCD four-circle goniometer (Enraf FR 90; Holand) around room temperature. The electronic density maps were transformed into the Q peaks using the SHELXS program based on the direct method which were assigned to the corresponding atoms according to their electron number [15]. Then the established structural models were refined using the SHELX-97 program to correct the atom types and clean the wrong atoms with large temperature vibration [16]. The H atoms were generated on the attached C atoms using the AFIX commands such as AFIX 43 and AFIX 137 [16]. The lattice DMF molecules are highly disordered due to their changeable locations around room temperature. They could not be found from the Q peaks of the Fourier electron density map in the crystal structure refinement. So we use the SQUEEZE manipulation embedded in the PLATON software to remove their contribution from the HKL file. The newly generated HKL file was used to refine the structures to get the CIF file with satisfied R factors [17]. Table 1 shows the crystallographic parameters and refinement results for compound **I**.

Supplementary material for structure **I** has been deposited with the Cambridge Crystallographic Data Centre (CCDC no. 1898532; deposit@ccdc.cam.ac.uk or http://www.ccdc.cam.ac.uk).

Computational details. The sorption and DMOL3 models embedded in the Material Studio 8.0 software was used to calculate the favorable location at zero loading, density distribution at saturated loading and the binding energy between the 5-FU molecule and the framework of Ia at zero loading [17]. The 5-FU molecule was drawn in the Material Studio 8.0 and then geometrical optimized using the DMOL3 model based on the B3LYP function, from which the EPS charge was calculated and then applied to the 5-FU molecule. The structure of **Ia** was derived from the crystal structure of **I** with removal of the coordinated water molecules. The network charge was calculated using the Qeq method based on the charged 1.1 method. The Fixed loading task was used to obtain the favorable location at zero loading, and the fixed pressure task was used to obtain of the 5-FU distribution in the framework of Ia at high loading. In simulation progress, the UFF force field was applied to all atoms.

MTT assay. FTC-133, BC-PAP and SW579 human thyroid cancer cells and one human normal cell were kept in the Roswell Park Memorial Institute (RPMI) 1460 medium, which contains streptomycin (80 μg/mL), penicillin (80 μg/mL) and fetal calf serum (10%). The complex **I** and 5-FU loaded **Ia** were made to stock solutions using the DMSO solution and then filtrated though the filter membrane. The stock solutions were diluted by the RPMI 1460 medium to various concentrations before the usage. After treatment of the cells with different concentrations of **I** and 5-FU loaded **Ia** for up to 96 h, MTT (0.5 mg/mL, 150 μL) solution was subsequently added and the mixture was further incubated for another 6 h. The formed

Table 1. Crystallographic data and structure refinement for complex **I**

Parameter	Value
Weight	904.21
T, K	293(2)
Crystal system	Hexagonal
Space group	$P6_522$
α, deg	90
β, deg	90
γ, deg	120
a, Å	17.96431(13)
b, Å	17.96431(13)
c, Å	22.1129(2)
Volume, Å^3	6180.13(11)
Z	6
ρ_{calcd}, g/cm^3	0.959
μ, mm^{-1}	7.749
θ Range for data collection, deg	6.948–135.754
Data/restraints/parameters	3721/0/163
GOOF	1.128
R_1, wR_2 factors ($I > 2\sigma(I)$)	0.0361, 0.1112
R_1, wR_2 factors (all data)	0.0380, 0.1133
Largest diff. peak and hole, e Å^{-3}	0.76 and –0.47
Flack parameter	0.228(9)

purple formazan crystals were dissolved via the addition of 60 μL of DMSO solution. A plate reader was used to record the emission intensity around 570 nm. In order to reduce the error, each experiment was parallelly done for 3 times and the results are expressed using the standard uncertainty.

RESULTS AND DISCUSSION

The title complex **I** was produced by a one pot solvothermal treatment of $Ba(NO_3)_2$ with a rigid tricarboxylic acid ligand H_3TATB in a mixture of H_2O and DMF at 120°C, whose structure has been established by SCXRD and phase purity has been validated by PXRD. Complex **I** is insoluble in common organic solvents, such as DMF, DMA and MeOH. The highly crystallized compound **I** was formulated as $[Ba(HTATB)(H_2O)_2](DMF)_4$ based on the analysis results from the SCXRD study and EA. Complex **I** belongs to the chiral hexagonal $P6_522$ space group and demonstrates a 3D channel-type network with nano-sized channels generated from the binding of the infinite $HTATB^{2-}$ ligands with the seven-coordinated Ba^{2+} ions. In the molecular unit there exist a half crystallographically independent Ba^{2+} ion, a half $HTATB^{2-}$ ligand, one disordered lattice DMF molecule as well as a coordinated H_2O molecule. The coordination environment of the Ba^{2+} ion is shown in Fig. 1a, which reveals that the pentagonal bipyramidal environment of Ba^{2+} ion is completed by seven O atoms from one coordinated water molecula and six carboxyl O atoms from six different $HTATB^{2-}$ ligands as calculated via the SHAPE 2.1 software [18]. The Ba–O bond lengths vary from 2.212(3) to 2.609(5) Å, which are in the normal range of the Ba–O bond distances observed in other Ba(II)-based MOFs constructed from the polycarboxylic acid ligand [19, 20]. The neighboring Ba^{2+} ions are connected with each other via the carboxylic groups along the c axis and the three carboxylic groups on the $HTATB^{2-}$ ligand show the same μ_2-η^1:η^1 mode (Fig. 1b). In this case, a 1D right-handed chain along a 6_1 axis was formed along the c axis which could be viewed as the $\{Ba(CO_2)_3(H_2O)\}_6$ cluster extending along the c axis via the carboxylic groups. The distance between the repeated $\{Ba(CO_2)_3(H_2O)\}_6$ cluster is 21.632(4) Å. A 3D porous network with 1D triangular windows along the c axis was formed by connection of the 1D right-handed chain by $HTATB^{2-}$ ligands, whose nano void spaces are occupied by the coordinated water molecules pointing toward the channel center. The window size for the triangular channel is 7.9 Å with the consid-

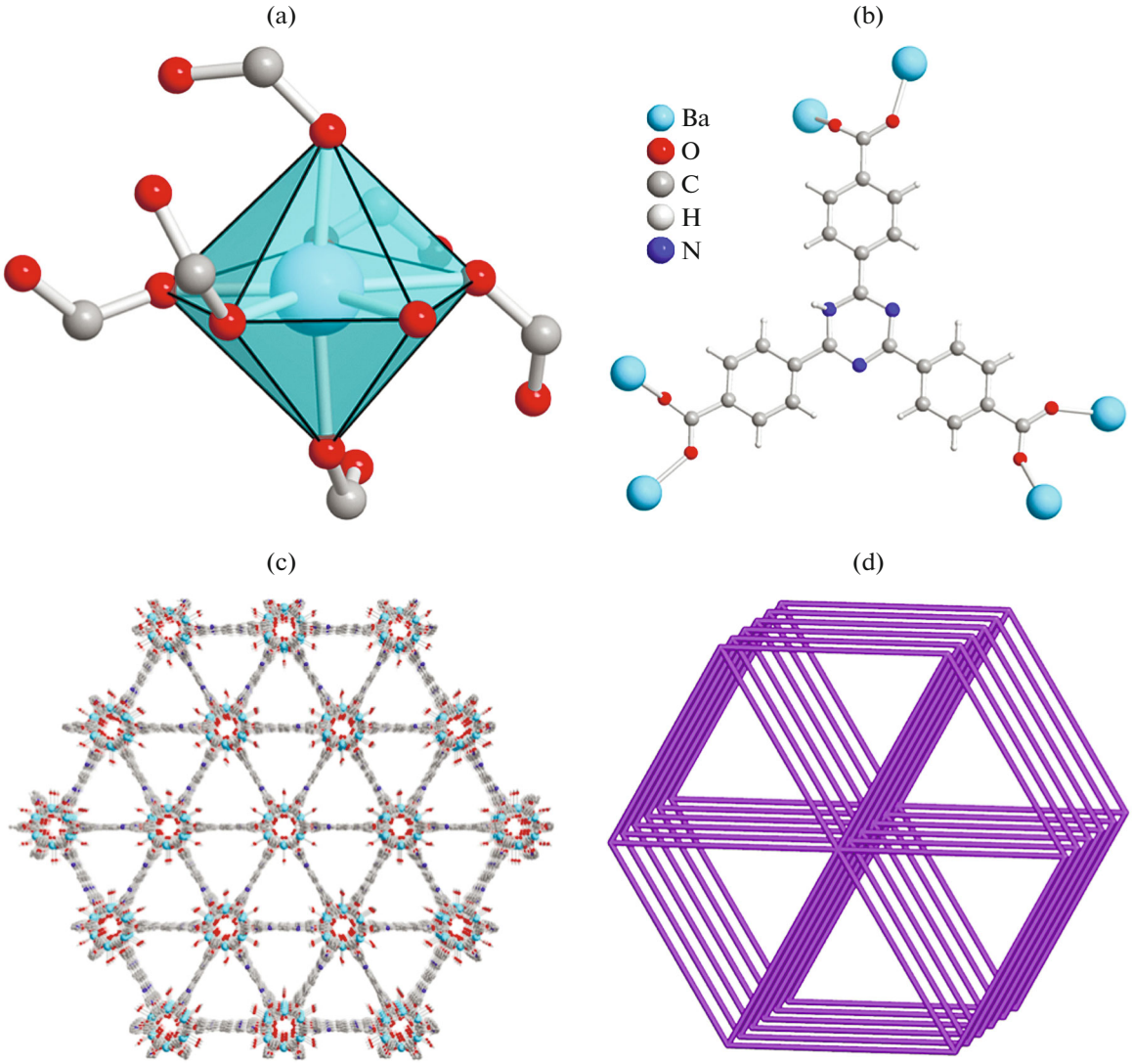

Fig. 1. View for the atoms that shape the coordination surrounding of Ba^{2+} ion (a); the μ_2-η^1:η^1 connection mode for the $HTATB^{2-}$ ligands of **I** (b); 1D channels of **I** with triangular windows (c); the 6-connected hxl-type topological network for **I** (d).

eration of the van der Waals radii of atoms (Fig 1c). From the viewpoint of net topology, this 3D framework could be viewed as a uninodal 6-connected hxl-type network with the point symbol of {3^6.4^6.5^3} (Fig. 1d). In this network, each $HTATB^{2-}$ ligand links two $\{Ba(CO_2)_3(H_2O)\}_6$ and each $\{Ba(CO_2)_3(H_2O)\}_6$ cluster connects with six $HTATB^{2-}$ ligands. The PLATON calculation results show that the solvent accessible void space for the framework of **I** is 58.3% (3567 of the 6180 $Å^3$) without considering the coordinated water molecules and the lattice free guests [21].

The phase purity of the as-prepared crystalline **I** was confirmed via the measurement of the PXRD pattern of the bulky as-synthesized **I** at room temperature, which indicates the bulky as-prepared crystalline products are in good phase purity as evidenced by the good agreement between the experimental and theoretical patterns (Fig. 2a).

TG stability of complex **I** was evaluated over the temperature range of 25–800°C. The TGA profile of **I** reveals a continuous 36.6% weight loss from room temperature to 246°C, corresponding to the removal of four lattice DMF and two coordinated water molecules (calcd. 36.4%, Fig. 2b). Then a short plateau appears till the temperature of 376°C followed by a sharp weight loss, indicating the framework of **I** decomposes. The morphology of the as-prepared samples of **I** was also probed via the scanning electron microscopy (SEM), which reveals their cube-shape crystalline products with the average size of 12 μm (Fig. 2c). As discussed in the crystal structure description section, compound **I** has triangular 1D channels along the *c* axis with a solvent accessible void of 58.3%,

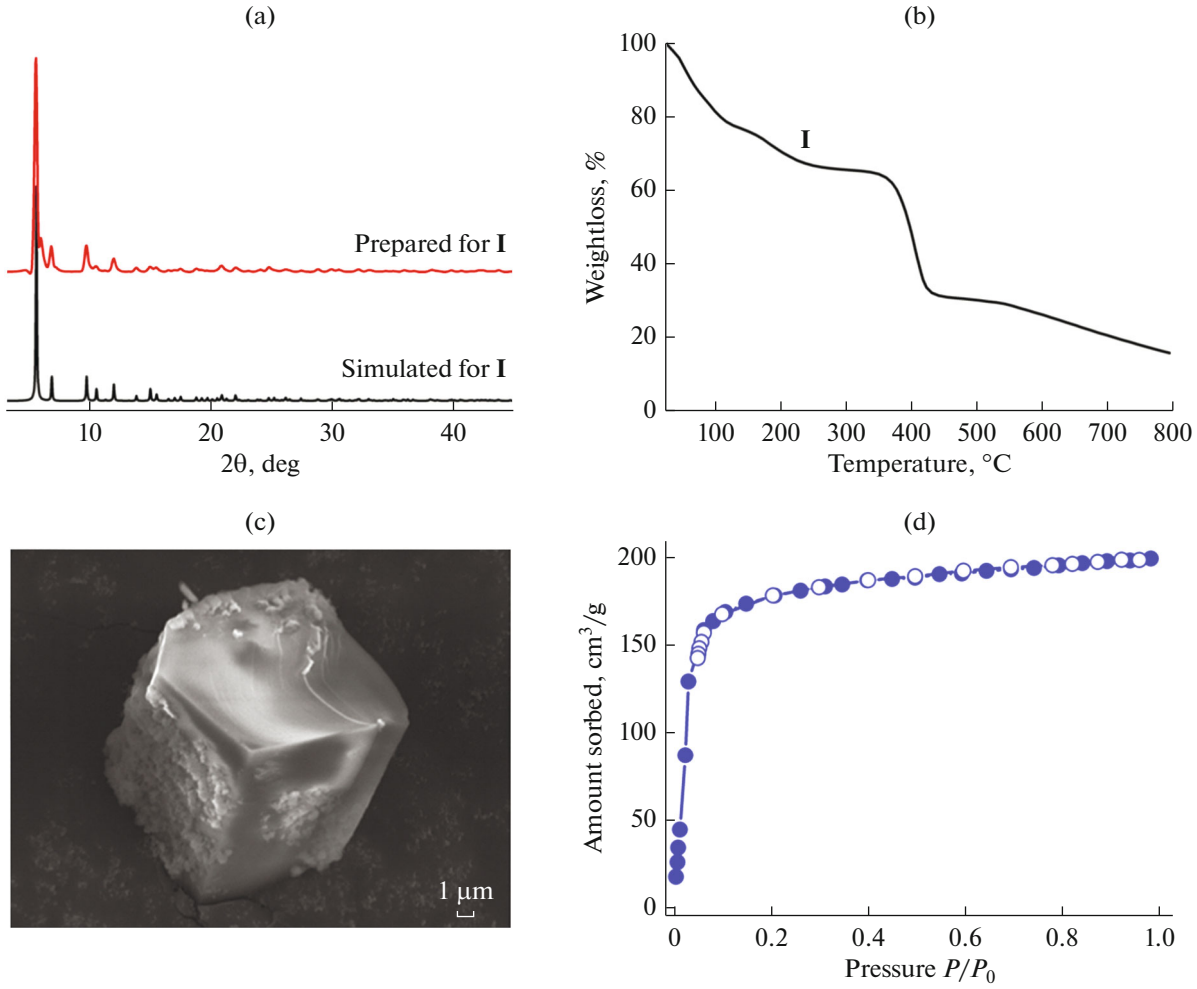

Fig. 2. The PXRD profiles of **I** (a); the TGA curve of **I** (b); the SEM image for **I** (c); the CO_2 sorption data for the activated **I** at 195 K (d).

which encourage us to probe its porosity via the gas sorption measurement. The the CO_2 sorption isotherm at 195 K of the solvent-free **I** (**Ia**) showed a type **I** isotherm without obvious hysteresis (Fig. 2d), which confirms that complex **I** is stable after guest removal and is micropore material. Based on the sorption data, the BET surface area was calculated to be 283 m^2/g (Fig. 2d).

As discussed above, the title complex **I** has considerable solvent accessible free volume and water occupied metal sites, which indicates that it could serve as a crystalline vessel for trapping the anticancer drug 5-FU. More importantly, compared with other toxic MOFs such as Cd-MOFs and Cr-MOFs, the Ba-MOF reported here is more environment-friendly and biocompatible. To evaluate the drug-loading capacity of the activated **I**, the as-prepared samples were soaked in 5 mL of MeOH solution with 30 mg of 5-FU with continually stirring, and UV-Vis spectra of the MeOH solution before and after the addition of activated **I** were recorded. An obvious decrease of adsorption intensity was observed after the crystalline samples of **Ia** were added, indicating the 5-FU molecules are trapped in the channels of **Ia**. Based on the intensity change of UV-Vis spectroscopy at 254 nm, the 5-FU loading capacity of **Ia** is 34.32 wt% (Fig 3a). The 5-FU delivery experiments were performed by dialyzing the 5-FU loaded **Ia** in the PBS buffer solution with the pH value of 7.4 at room temperature and the amount of 5-FU released was determined by HPLC. As shown in the Fig 3b, the 5-FU release profile reveals a sustaining release without "burst effect". It could be observed that nearly 61% of the loaded 5-FU molecules were released within 95 h with a relative steady release speed (Fig 3b). In the same time, three different drug release stages could be distinguished. In the first stage (from 0 to 11 h), about 22% of the loaded 5-FU molecules were released. Then from 12 to 58 h and 58 to 95 h, about 28 and 23% of the trapped 5-FU molecules were released in the latter two stages. As discussed in the structural description section and confirmed by the CO_2 sorption at 195 K, the triangular

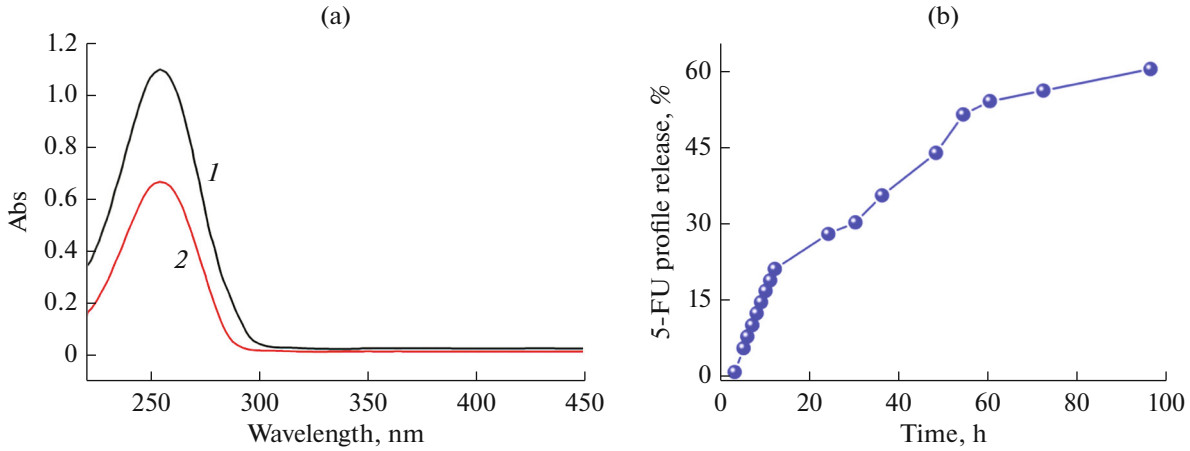

Fig. 3. The intensity change of the UV-Vis spectra for the 5-FU–MeOH solution before (*1*) and after (*2*) the addition of complex **Ia** (a); the release profile of 5-FU loaded **Ia** (b).

window size of **I** is larger than the molecular size of the 5-FU drug molecule (7.9 Å vs. 5.3 Å). The strong interactions between the open metal sites of **Ia** and the donor atom sites such as F and O atoms of the 5-FU may result in the observed slow 5-FU release speeed.

To make a better understand of the 5-FU loading process in the solvent-free framework of **I**, the molecular dynamics (MD) and the configurational bias Monte Carlo (CBMC) calculations were carried out to get a deep insight on the preferential location and distribution of 5-FU molecules in the framework of **I** at zero loading and saturated loading at room temperature. The fixed pressure task of the sorption module embedded in the Materials Studio 6.0 was used to determine the loading capacity of 5-FU molecules in the framework of **I** at 1 bar and room temperature. As demonstrated in Fig. 4a, the calculated fixed pressure map indicates that the activated **I** could uptake 8 5-FU molecules per four unit cells, corresponding to 32.4 wt % (~0.26 g/g), which is similar to the value calculated from the UV-Vis spectroscopy and this is also comparable with those porous MOFs targeted for the 5-FU delivery. Furthermore, there are H-bond interactions between the 5-FU molecules and the N atoms on the $HTATB^{2-}$ ligand with the N–H···N bond lengths varying from 2.429 to 2.726 Å, which is very important for slowing down the drug releasing rate, leading to the drug sustained release. The density distribution also shows that the 5-FU molecules mainly locate neighboring to the N atoms and the open metal sites near the Ba^{2+} ions of the $HTATB^{2-}$ ligands, indicating the importance of H-bond interaction along with the open metal sites for the accommodating 5-FU molecules in the framework of **I** (Fig. 4b). In order to get the favorable conformation of 5-FU at zero loading, the fixed loading task of the sorption module embedded in the Materials Studio 6.0 was used to calculate the location of 5-FU in the framework of **I** in which the loading was set to 1. As shown in Fig. 4c, the snapshot shows that one 5-FU locates near the $HTATB^{2-}$ ligand with two short interactions: one is the N–H···N H-bond interaction with the distance of 2.897 Å, and the other is the Ba–F interaction with the distance of 3.108 Å (Fig 4c). The binding energy for the two short interactions via the DFT calculation is 63.9 kJ/mol, which highlight the importance of H-bond and donor-acceptor interactions for the creation of strong interaction between the framework of **I** and the 5-FU molecules [22].

The successful accommodation of 5-FU molecules into the nano spaces of **Ia** promotes us to study the anticancer activities of the 5-FU loaded **Ia**. The in vitro cell viabilities of pure compound **I** against the human oral epidermal cells (normal cells) with the concentration ranging from 10 to 120 μg/mL were studied via the MTT assay to confirm the low cytotoxicity of the carrier **I**. The cell viabilities were plotted in Fig. 5a, which shows that the above 80% of the normal cells are alive even at a concentration of 120 μg/mL of **I**, so the carrier **I** shows low cytotoxicity toward the human normal cell lines. The anti-thyroid cancer activity of the 5-FU loaded **Ia** were studied via the MTT assay against three human thyroid cancer cells (FTC-133, BC-PAP and SW579) with the carrier **I** as the negative control. The anticancer activities were accessed by the IC_{50} values which are plotted in the Fig. 5b. The IC_{50} values for the carrier **I** are all far above 100 μM against three human thyroid cancer cells, which indicate the carrier **I** has no anticancer activity. In comparison, the IC_{50} value for the 5-FU loaded **Ia** toward the three cancer cell lines varying from 24 to 33 μM, reflecting that the cytotoxicity of compound **I** toward the cancer cells are greatly enhanced after trapping the 5-FU in the nano pores of **Ia**. The above results also show that the complex **I** might be a good candidate for the anticancer drug 5-FU loading and release in the future.

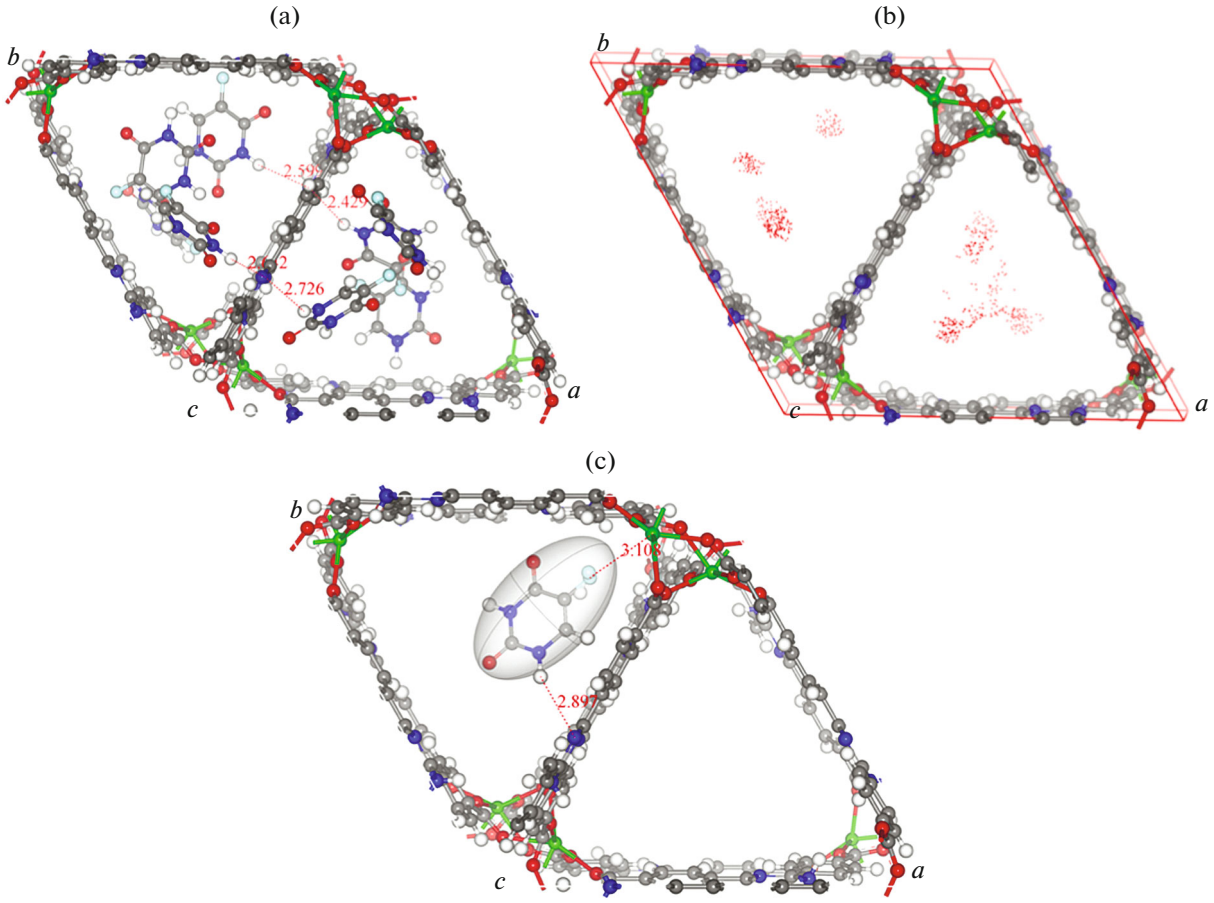

Fig. 4. The conformation of 5-FU in the framework of **I** at 298 K and 1 bar (a); the map showing the density distribution of 5-FU at saturated loading (b); the favorable location of 5-FU at zero loading (c).

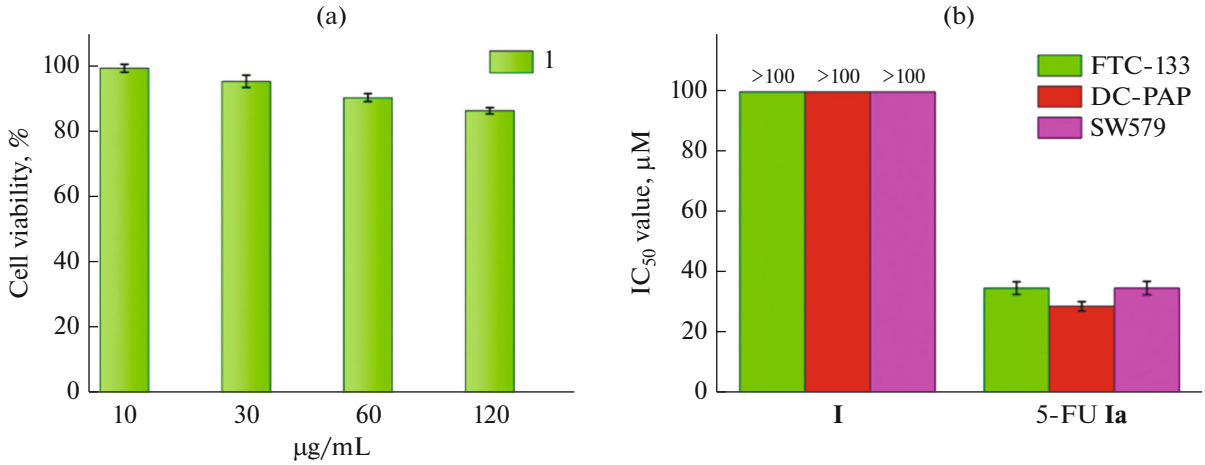

Fig. 5. Cell survival of the oral epidermal cells after treatment with **I** at different concentrations (a); the cytotoxicity of 5-FU loaded **Ia** on FTC-133, BC-PAP and SW579 cells (b).

In summary, a new three-dimensional porous Ba(II)-organic framework with the formula of $[Ba(HTATB)(H_2O)_2](DMF)_4$ (**I**) has been solvothermally produced by reaction of $Ba(NO_3)_2$ with a rigid tricarboxylic acid ligand 4,4',4"-s-triazine-2,4,6-triyl-tribenzoic acid (H_3TATB) in the mixture of H_2O and DMF. In light of its large inner spaces as well as widely distributed open metal sites, the desolvated **I** (**Ia**) was

used as a crystalline vessel for trapping the anticancer drug 5-fluorouracil, which has been investigated both experimentally and computationally. In addition, the cytotoxicity of compounds **I** and 5-FU loaded **Ia** have also been evaluated using MTT assay on three human thyroid cancer cells (FTC-133, BC-PAP and SW579) and one human normal cell line, and the experimental results reveal that the carrier **I** shows little toxicity to the human normal cell lines and the 5-FU loaded **Ia** demonstrate promising anticancer activity against the cancer cell tested.

REFERENCES

1. Twombly, R., *J. Natl. Cancer Inst.*, 2005, vol. 97, p. 330.
2. Debatin, K.M. and Krammer, P.H., *Oncogene*, 2004, vol. 23, p. 2950.
3. Di Fiore, F., Blanchard, F., Charbonnier, F., et al., *Br. J. Cancer.*, 2007, vol. 96, p. 1166.
4. Vallet-Regí, M., Balas, F., and Arcos, D., *Angew. Chem. Int. Ed.*, 2007, vol. 46, p. 7548.
5. Zhou, H.C., Long, J.R., and Yaghi, O.M., *Chem. Rev.*, 2012, vol. 112, p. 673.
6. Long, J.R. and Yaghi, O.M., *Chem. Soc. Rev.*, 2009, vol. 38, p. 1213.
7. Duan, C., Li, F., Yang, M., et al., *Ind. Eng. Chem. Res.*, 2018, vol. 57, p. 15385.
8. Niu, L., Xu, J.L., Yang, W.L., et al., *Sci. Adv. Mater.*, 2019, vol. 11, p. 466.
9. Yang, Y.Y., Kang, L., and Li, H., *Ceram. Int.*, 2019, vol. 45, p. 8017.
10. Zhao, H., Mu, X., Zheng, C., et al., *J. Hazard. Mater.*, 2019, vol. 366, p. 240.
11. Chen, D.M. and Zhang, X.J., *CrystEngComm*, 2019, vol. 21, p. 4696.
12. Horcajada, P., Gref, R., Baati, T., et al., *Chem. Rev.*, 2012, vol. 112, p. 1232.
13. Horcajada, P., Serre, C., Maurin, G., et al., *J. Am. Chem. Soc.*, 2008, vol. 130, p. 6774.
14. Wang, L., Zheng, M., and Xie, Z., *J. Mater. Chem., B.*, 2018, vol. 6, p. 707.
15. Sheldrick, G.M., *SHELXS-86, Program for Crystal Structure Solution*, 1986.
16. Sheldrick, G.M., *Acta Crystallogr., Sect. A: Found. Crystallogr.*, 2008, vol. 64, p. 112.
17. Chen, D.M., Liu, X.H., Tian, J.Y., et al., *Inorg. Chem.*, 2017, vol. 56, p. 14767.
18. *SHAPE: Program for the Stereochemical Analysis of Molecular Fragments by Means of Continuous Shape Measures and Associated Tools*, Barcelona (Spain): Univ. of Barcelona, 2010.
19. Spek, A.L., *Acta Crystallogr., Sect. C: Struct. Chem.*, 2015, vol. 71, p. 9.
20. Kotzabasaki, M. and Froudakis, G.E., *Inorg. Chem. Front.*, 2018, vol. 5, p. 1255.
21. Cao, K.L., Xia, Y., Wang, G.X., et al., *Inorg. Chem. Commun.*, 2015, vol. 53, p. 42.
22. Zhang, X., Huang, Y.Y., Zhang, M.J., et al., *Cryst. Growth Des.*, 2012, vol. 12, p. 3231.